Marine Boundary Layer Dynamics During ASTEX

CHRISTOPHER S. BRETHERTON

Atmospheric Science Department, AK-40, University of Washington, Seattle, WA 98195

Abstract

The Atlantic Stratocumulus Transition Experiment (ASTEX), conducted in June 1992 in the central North Atlantic Ocean, provided a variety of coordinated measurements of cloud-topped marine boundary layers (MBL's) using aircraft, ground-based and remote sensing techniques. Soundings from two island stations and four ships participating in the experiment were incorporated into operational ECMWF analyses for the period to provide as good as possible a regional definition of the large scale synoptic meteorology and particularly the mean vertical velocity. ECMWF forecasts were also used in the field for trajectory analysis. An extensive set of ceilometer and satellite retrievals of cloud cover, meteorological, radiation and chemical measurements was obtained during ASTEX. Two Lagrangian experiments, in which boundary layer airmasses were followed nearly continuously for 36-48 hours, provided unprecedently detailed pictures of a clean, shallow drizzly and a dirty, deep, cumuliform MBL

The MBL in the ASTEX region showed substantial synoptic variability and a significant diurnal cycle with an early morning maximum in cloud cover. The thermodynamic structure was rarely 'well-mixed' in the vertical, and typically was similar to that of a trade-cumulus cloud regime except that a saturated stratocumulus cloud layer was common under the trade inversion. Drizzle processes seemed to substantially affect both the mean cloud properties and mesoscale organization of the MBL cloudiness. An LES model can reproduce many features of this cloud regime.

1. Objectives and Overview of ASTEX

Figure 1, from Klein and Hartmann (1993), shows a 40 year annually averaged climatology of boundary layer stratus cloud amount (including fog ,nimbostratus, and mixed stratus and cumulus, as well as solid nonprecipitating stratus) from routine surface-based synoptic reports. Figure 2, from the same source, shows cloud radiative forcing deduced in the Earth Radiation Budget Experiment (ERBE). One sees a strong correlation between regions of substantial negative cloud radiative forcing (where the cloud albedo effect is stronger than its greenhouse effect, providing a cooling influence on climate by reducing the net downward flux of radiation at the top of the atmosphere) and regions of large MBL stratus cloud cover. Evidently, an accurate parameterization of MBL cloud is crucial to long-term climate prediction as it will affect sea-surface temperature. In short or medium range forecasts, substantial forecast errors can be traced to MBL's which develop incorrect depth or cloud cover over data-sparse ocean regions and then advect over the continents.

Over the cool water off the west coasts of the Americas and Africa east of the subtropical highs, extensive regions of the oceans which are blanketed by nearly solid stratocumulus for much of the year. As this air advects westward and equatorward in the trade winds, there is a climatological transition to trade cumulus clouds with lower fractional cloud cover and a deeper boundary layer ; we will call this transition the STT (*S*tratocumulus to *T*rade cumulus *T*ransition.) .

There is a qualitative change in the boundary layer structure and dynamics between the two endpoints of this transition that is intimately linked with cloudiness. Shallow coastal stratocumulus layers are generally observed to consist of convective circulations which extend through the entire depth and breadth of the layer. They are fairly *well mixed*, so thermodynamic quantities conserved following adiabatically displaced fluid parcels, such as the moist static energy or mixing ratio, are observed to have small variations both in the vertical and the horizontal (Roach *et al* 1982). Trade cumulus layers, on the other hand, are not well mixed. The archetypical trade cumulus boundary layer consists of a fairly well-mixed convecting *subcloud layer*, a *transition layer* at the cumulus cloud base generally marked by a weak inversion and a decrease in mixing ratio, and

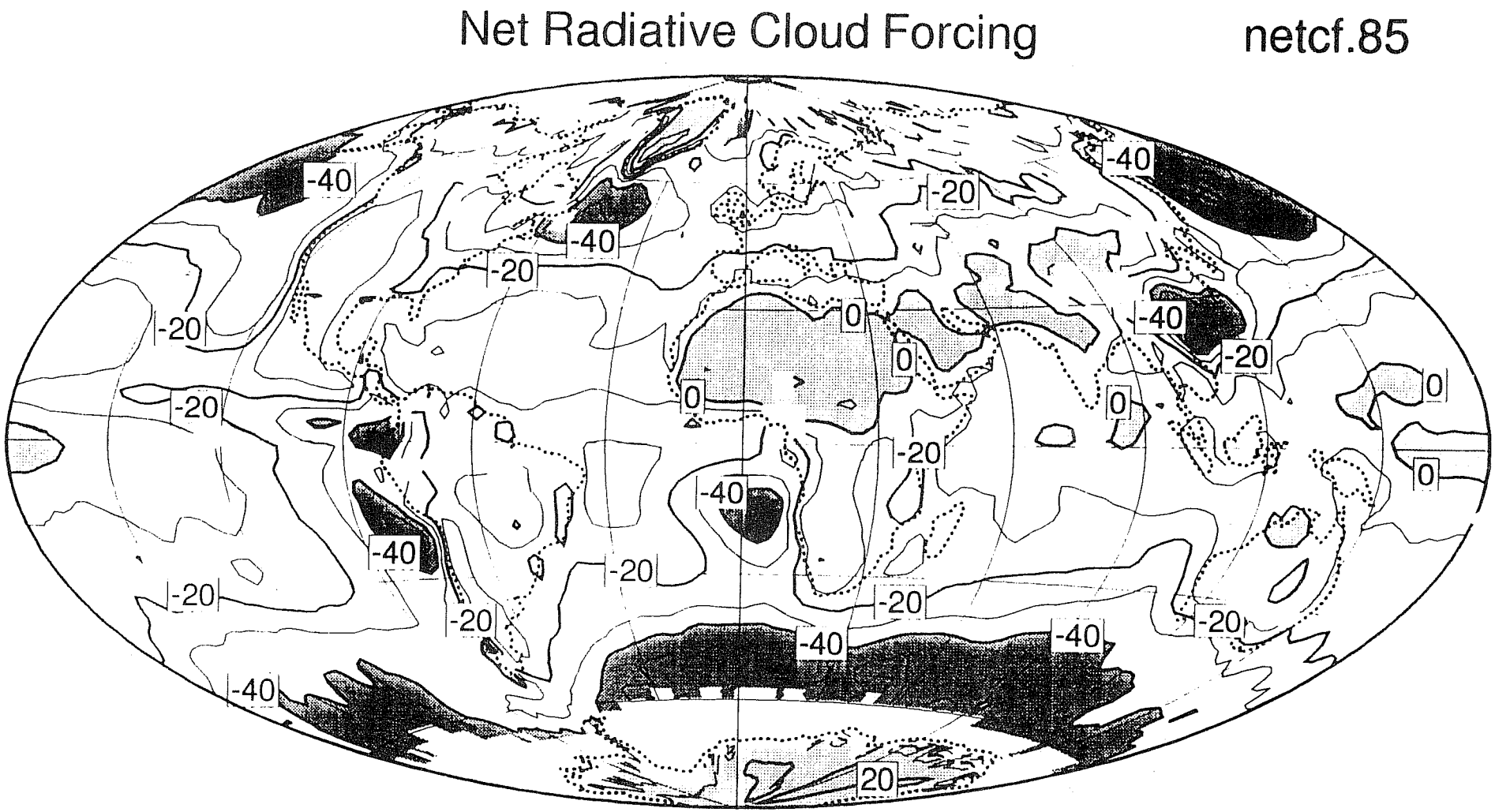

Fig. 1 Annually averaged boundary layer stratus cloud amount from surface synoptic reports (from *Klein and Hartmann*, 1993).

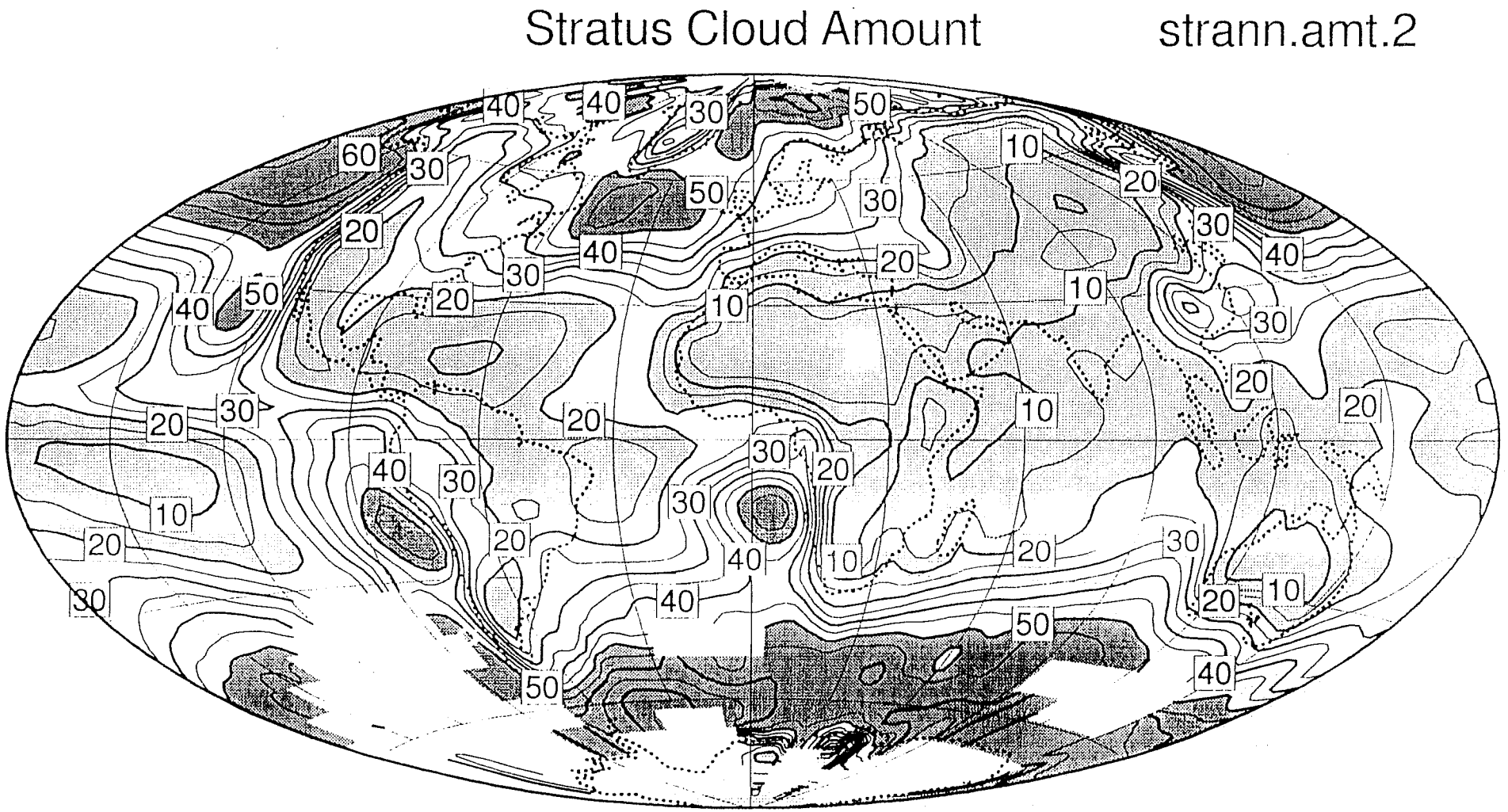

Fig. 2 Net cloud radiative forcing in 1985 from ERBE data (from *Klein and Hartmann*, 1993).

a *cumulus layer* in which the mean mixing ratio decreases with height, but the mean relative humidity tends to remain between 80-95%, and the stratification lies between dry and moist adiabatic (Malkus 1958, Augstein *et al* 1974, Betts and Albrecht 1987). The cumuli penetrate into a *trade inversion* of strength 2-5 K which is generally 100-400 m thick.

The STT is still poorly understood and poorly or artificially parameterized in many climate and forecast models. The main goal of ASTEX was to provide a more complete physical description of the STT. Figure 3a shows the ECMWF analyzed June 1-23 mean isobars, 10 m wind vectors and sea-surface temperature (SST) for June 1-23, 1992 in the ASTEX area. Figure 3b shows the ECMWF analyzed 850 hPa mean winds and vertical velocity. Superimposed is the 'ASTEX triangle' formed by two island stations, Santa Maria (Azores) at the northwest, and Porto Santo (Madeiras) at the east, and a ship stationed at the southwest. Both islands were less than 20 km long and had 500-700 m high topography. The observing sites were chosen on the upwind side of each island, but island-driven diurnal effects were unavoidable. East of the Azores High, northerly flow with typical wind speeds of 5-10 m s^{-1} and weak subsidence typically prevailed. A daily summary of the field operations, the synoptic situation, soundings and satellite imagery is available from B. A. Albrecht of the Department of Meteorology, Pennsylvania State University (Bluth and Albrecht 1993).

A trade inversion could usually be identified between 800 and 900 hPa. However, substantial synoptic variability was the rule. Figure 4 shows four soundings from the morning of 15 June which show a shallow well-mixed stratocumulus-capped boundary layer at Santa Maria, a much deeper trade cumulus layer with a suggestion of saturation at 850 hPa at Porto Santo, a classic trade-wind boundary layer sounding at the R/V Valdivia at the SW corner of the triangle, and a shallow but unsaturated MBL above the R/V Le Suroit, only 60 km from Santa Maria. Figure 5 shows time series of inversion base pressure and the lifted condensation level (LCL) of 1000 hPa air from sonde ascents. Here an inversion in a significant-level sounding was identified as the lowest layer in which the temperature rose by at least 1 K between successive significant levels, if such existed. Rapid and large changes in inversion pressure were associated with both horizontal and

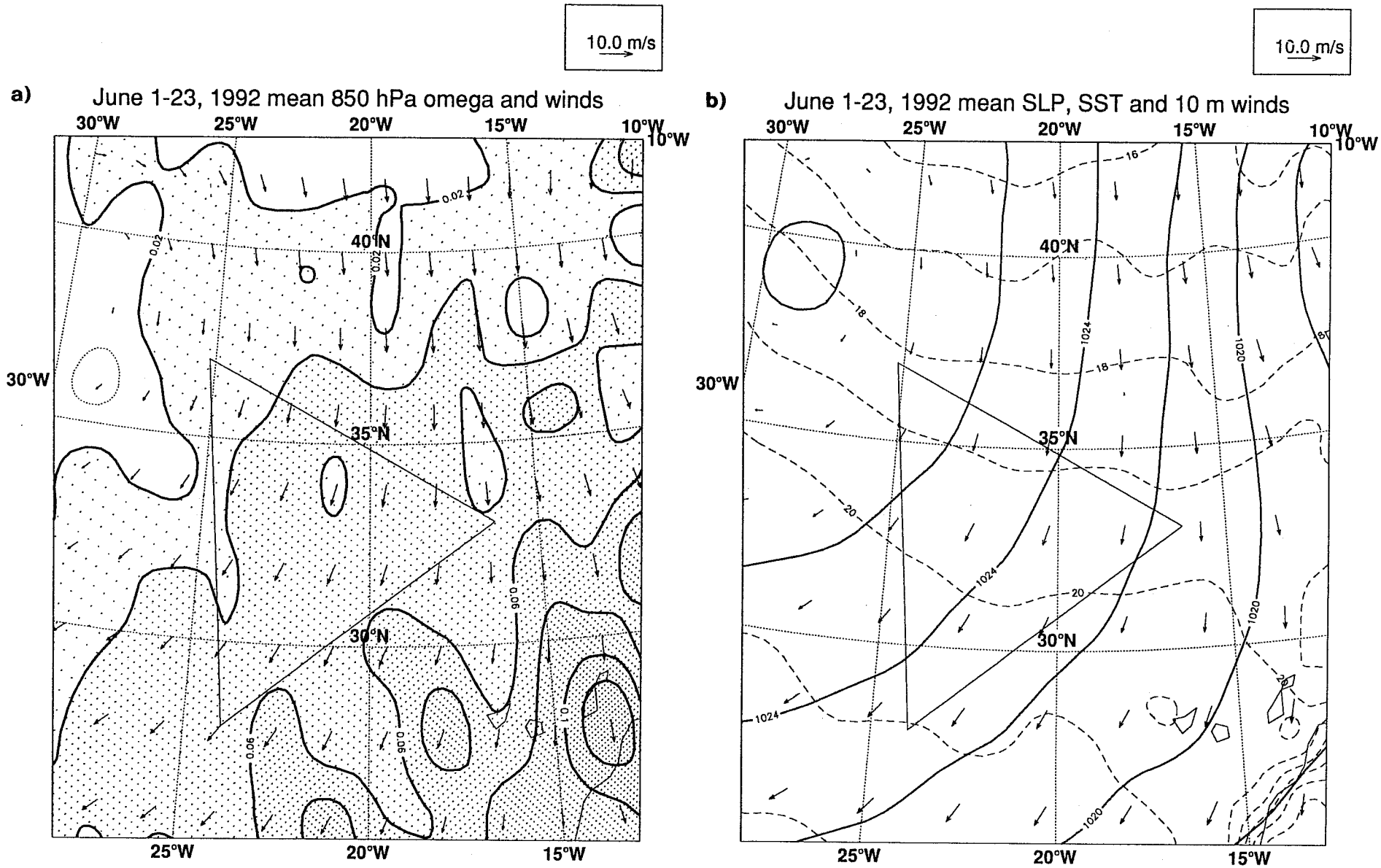

Fig. 3 ECMWF June 1-23, 1992 mean (a) sea level pressure (solid), SST (dashed) and winds, and (b) 850 hPa mean $\bar{\omega}$ (Pa s^{-1}) and winds.

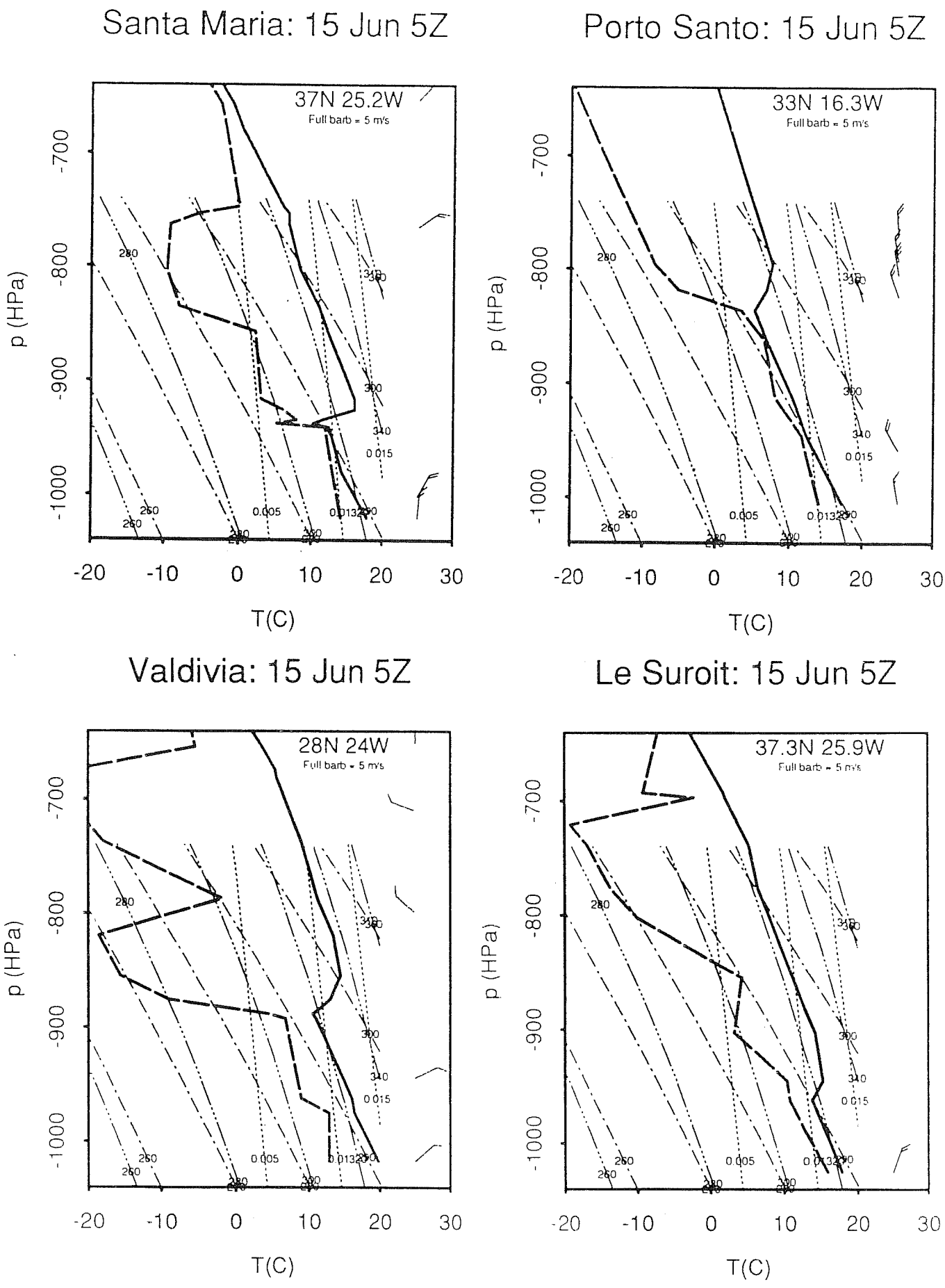

Fig. 4 ASTEX significant-level soundings for 06Z 15 June.

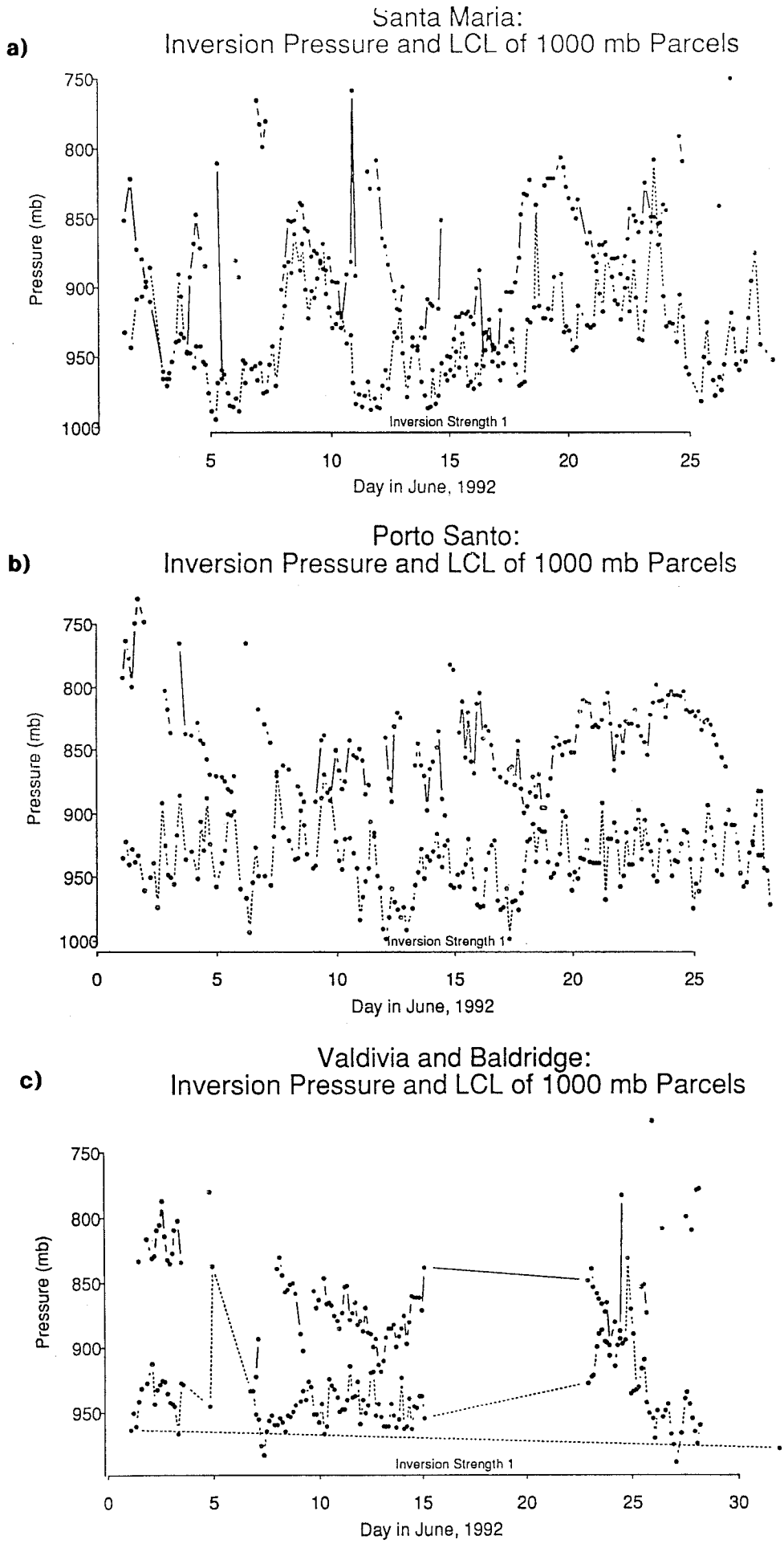

Fig. 5 Time series of inversion base pressure (when an inversion was diagnosed) and 1000 mb lifted condensation level at (a) Santa Maria, (b) Porto Santo and (c) 28 N, 24 W.

vertical advection in the south fringes of frontal systems, especially at Santa Maria. Occasionally the flow would even reverse direction, blowing from warmer SST's; on several occasions this led to fog formation. The diurnal cycle of 1000 hPa LCL was rather stronger at the island stations, especially Porto Santo, than at the ship.

A preliminary comparison of the ECWMF analyses available in the field and the soundings at the triangle vertices at standard levels showed quite good agreement with little systematic bias. Figure 6 shows the scatter of differences between analyzed and measured temperature and dew-point at Santa Maria at 1000, 850 and 700 hPa.

Because ASTEX was held in collaboration with an atmospheric chemistry experiment, the Marine Aerosol and Gas Exchange experiment, or MAGE, ECMWF analyses were used in the field to generate back-trajectories from observing sites. Aerosol and chemical characteristics, cloud droplet numbers, and drizzle frequency were highly dependent on the history of the boundary layer airmass during the previous three days. Since aerosol is constantly entrained into the boundary layer, trajectories above the boundary layer were also relevant. Figure 7 shows surface and 700 hPa isentropic back-trajectories from 12Z 15 June originating from the three corners of the ASTEX triangle and the center of the NE leg. Note that at this time, surface air in the southeast part of the triangle was coming from Europe, while at Santa Maria, air was still circulating from the northwest around the Azorean high. The 700 hPa back-trajectories from the southwest corner were frequently from the west even though the surface air was in steady northeast trades.

2. The Lagrangian Experiments

The large effects of horizontal advection on thermodynamic, microphysical and chemical characterisitcs of the MBL make it difficult to compare observations at a fixed site with process models. In ASTEX/MAGE, two 'Lagrangian' experiments were performed in which boundary layer air columns were continuously sampled by boundary layer aircraft for 36-48 hours. Due to the limited range of the aircraft it was important to have a trajectory which started well upstream of the aircraft base at Santa Maria, came close to Santa Maria but did not go over any island (which would con-

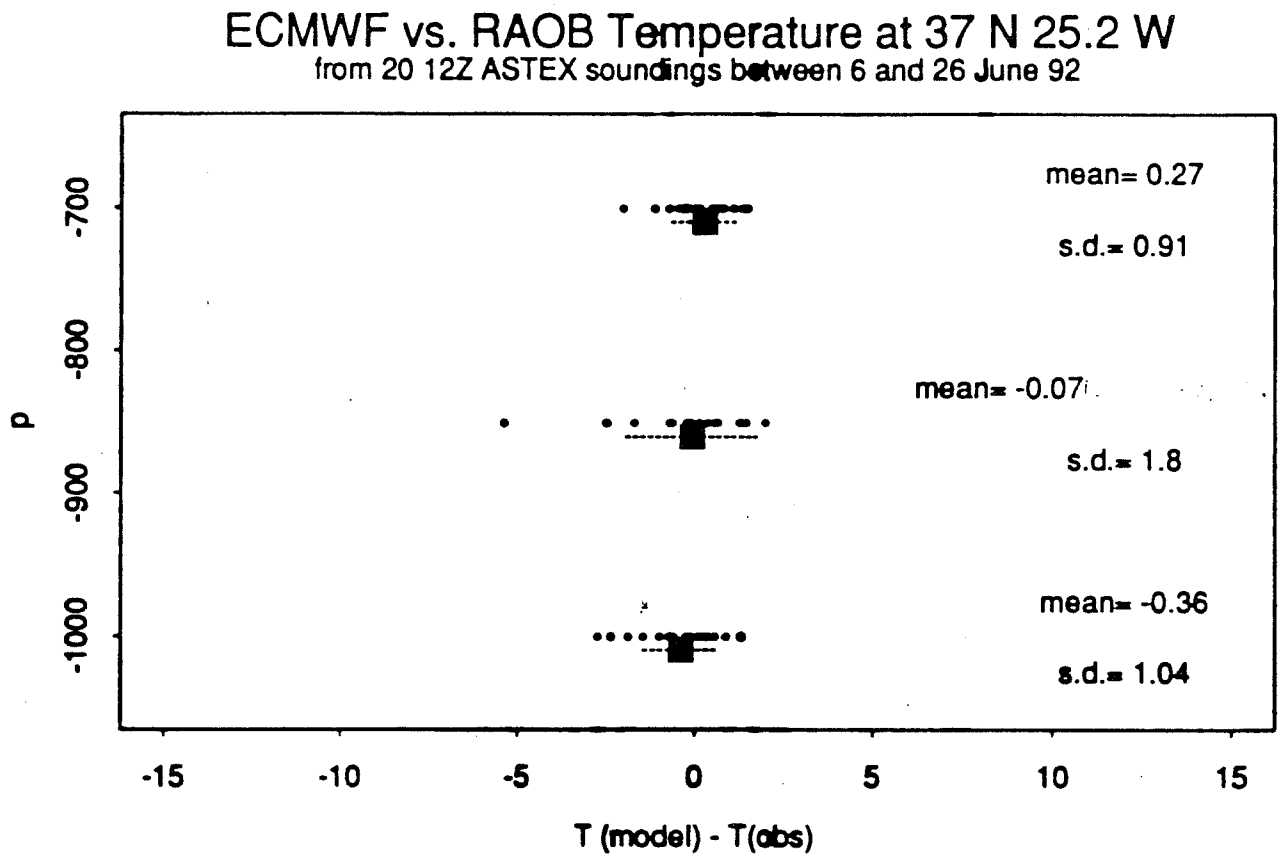

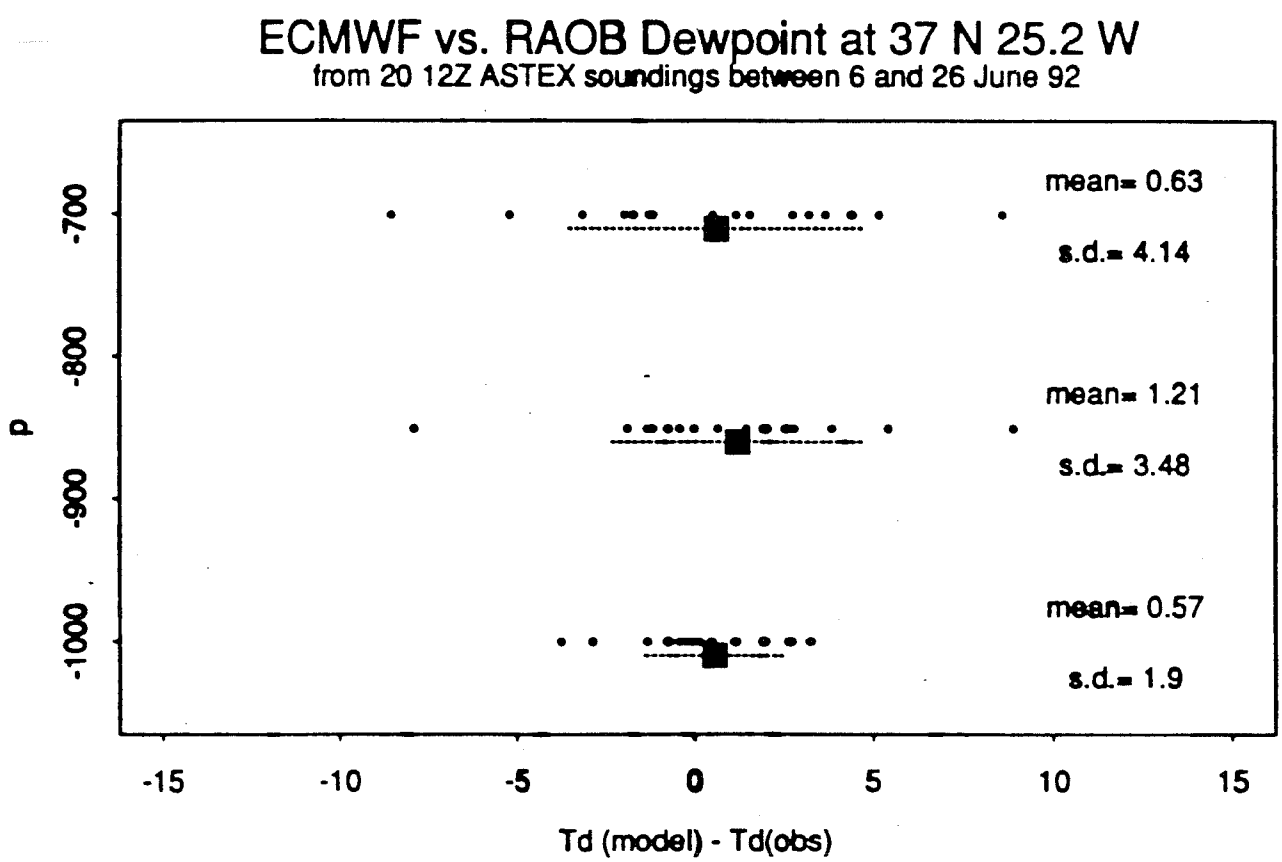

Fig. 6 Scatterplot of differences between ECMWF analyzed and radiosonde temperature and dewpoint at Santa Maria at 1000, 850 and 700 hPa. For each level, the heavy square is the mean bias and the dotted line segment extends one standard deviation in each direction.

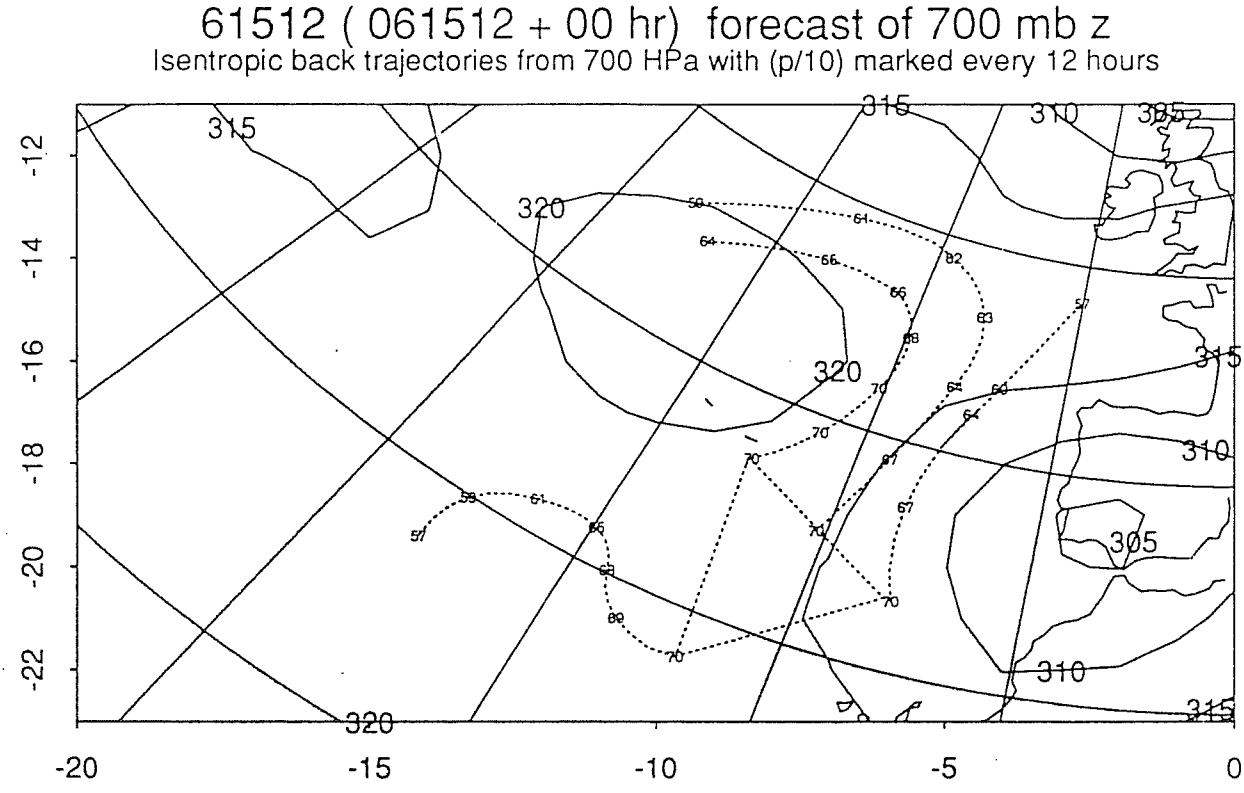

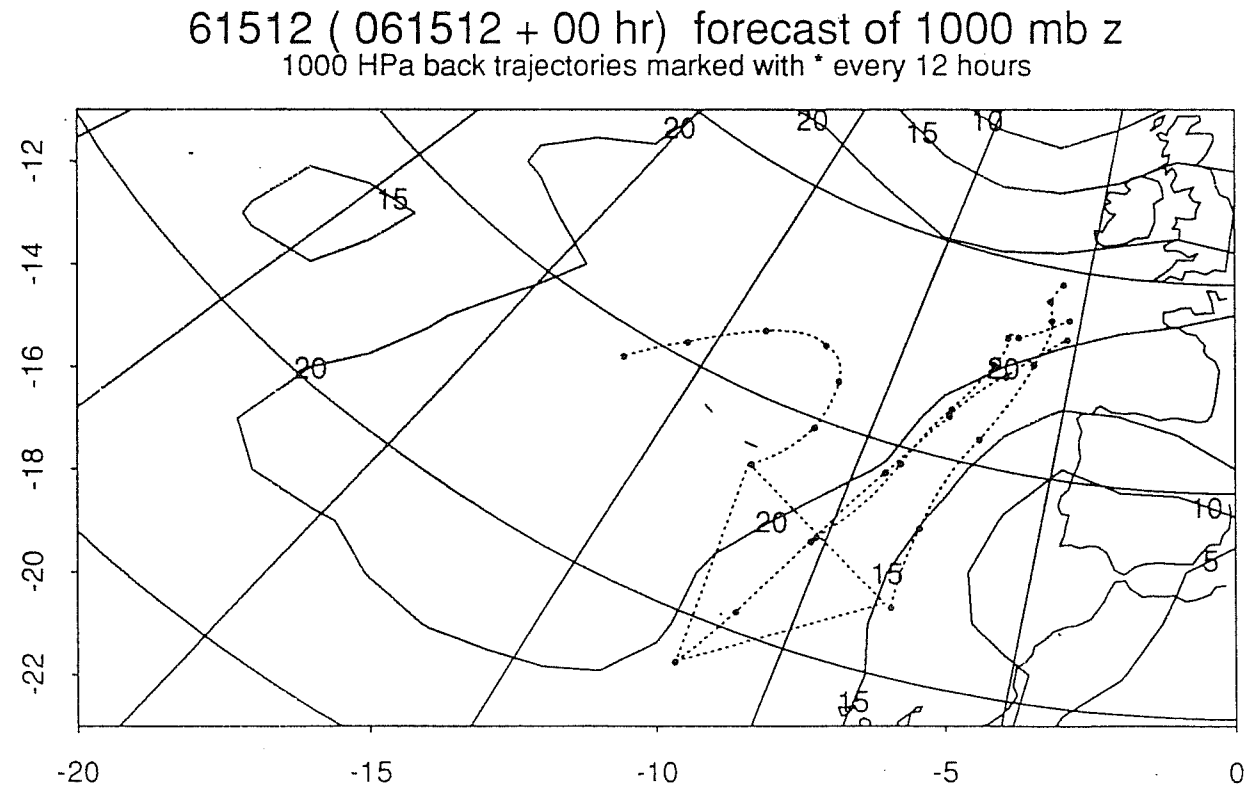

Fig. 7 Surface and 700 hPa back-trajectories from 12Z 15 June originating from the three corners of the ASTEX triangle and the centre of the NE leg. The 700 hPa trajectories are isentropic except for an assumed cooling of 2 K day^{-1} along the trajectory. The dots on the surface trajectory and the numbers (=pressure/10) on the 700 hPa trajectory show the position every twelve hours.

taminate the chemistry) and then went downwind. Balloons ballasted to initially rise to about 750 m and equipped with GPS position-finding equipment and a radio transmitter which could broadcast this position to aircraft within 150 km were used to follow the boundary layer air. Using trajectory forecasts using ECMWF, the R/V Oceanus was positioned upwind and released the balloons , then steamed behind the balloons to make ocean chemistry measurements, and the R/V Malcolm Baldridge sampled the air at the end of the trajectory. Three aircraft, the NCAR Electra, the UKMRF C130, and the University of Washington C131a were flown in sequence to provide a continuous set of soundings and legs at various heights in and somewhat above the boundary layer, making turbulence, microphysical, radiation and chemical measurements. The experiments were largely extremely successful but some complications emerged. The balloons proved very sensitive to the loading by drizzle wetting, and all sank within eight hours in Lagrangian 1, so MBL average winds from the aircraft had to be used from then on. Furthermore, drizzle and a low cloud base in Santa Maria forced observations to be suspended for 12 hours in the latter half of Lagrangian 1. During Lagrangian 2, one of five balloons was tracked for the entire 36 hour period, and aircraft observations were continuous. In addition, the low wind speeds made it possible for the Oceanus to steam downstream staying only slightly behind the balloons, so three-hourly radiosonde data from the Oceanus provided information on the mid and upper troposphere following the trajectory and was also incorporated into ECMWF analyses.

Figure 8 shows a schematic of the contrasting boundary layer development during the two Lagrangians. In Lagrangian 1, the MBL was initially only 60 hPa deep and was formed of pristine marine air. For the first day this MBL was capped by solid drizzling stratocumulus. Toward the end of the study period, the air moved under an upper level subtropical low and the MBL deepened, becoming more cumuliform. In Lagrangian 2, the MBL was 200 hPa deep throughout the period, with a 150 hPa deep cumulus cloud layer and patchy stratus, mainly beneath the very strong trade inversion. The stratus cloud amount was much higher at night. The cumuli had vigorous updrafts up to 5 m s^{-1}, but only a little precipitation fell; the air was relatively dirty since it had recently streamed off of Europe, and cloud droplet concentrations were typically 150 cm^{-3} as opposed to 50

Lagrangian 1 (16Z 12 June-16Z 14 June)

- Shallow, clean CTBL with drizzle, moderately strong winds.

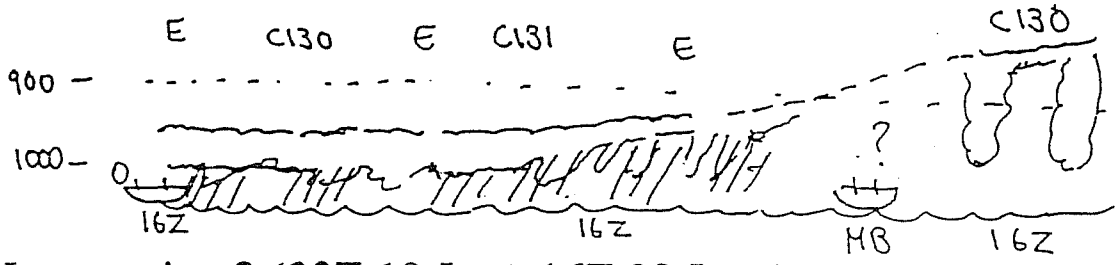

Lagrangian 2 (22Z 18 June-16Z 20 June)

- Deeper decoupled, largely nonprecipitating CTBL, moderately polluted, lighter winds.

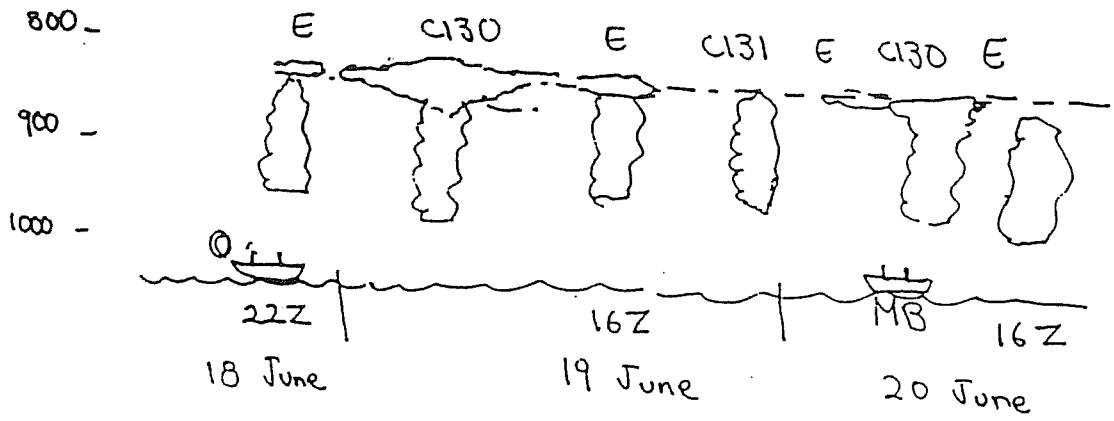

Fig. 8 Summary of the two ASTEX Lagrangain experiments. The symbols E, C130 and C131 refer to times of aircraft coverage by each aircraft, MB is the R/V Malcolm Baldridge, and cloud coverage and drizzle are indicated.

cm^{-3} in Lagrangian 1. Figure 9 shows the trajectories and the location of the 18 aircraft soundings taken during each Lagrangian.

Figure 10 shows aircraft soundings of θ and q_v at the beginning and end of Lagrangian 1, showing the transition from a well-mixed stratocumulus capped MBL to a trade cumulus-like boundary layer with some stratocumulus under the trade inversion. Figure 11a shows a pressure-time section of mixing ratio for Lagrangian 2. Although there is some mesoscale variability, the structure beneath the trade inversion was reproduced in all 18 soundings, with an approximately 2 g kg^{-1} decrease of mixing ratio in the transition layer near the cumulus cloud base, and relatively well mixed layers above and below. The mixing ratio (and ozone) above the inversion varied substantially with time. Figure 11b, wind vectors averaged over 40 hPa intervals from all the Electra soundings, shows that within the boundary layer there was little vertical wind shear , but at the inversion there was often substantial wind shear that brings different free tropospheric air over the same MBL airmass. The aircraft data analysis for ASTEX has only just begun and there should soon be many more results on the microphysical and radiative properties of the Lagrangian MBL's.

An attractive feature of the Lagrangian experiments, especially for chemists, was the simplicity of budget analysis when horizontal advection need not be considered. There remains one important unknown, the mean vertical velocity, which is necessary to deduce entrainment rates from the downstream changes in inversion height. Entrainment rates were measured directly during ASTEX on the Electra by finding the downward ozone flux from eddy correlation measurements using fast ozone sensor and turbulence instrumentation, and dividing by the ozone jump. The ozone jumps duing the Lagrangians frequently showed large mesoscale variability and were not always present, so only one trustable measurement for each Lagrangian was obtained. Similarly, a budget of water vapor can (if the precipitation loss is known or ignored) be used to back out entrainment rates, but for Lagrangian 1, the precipitation flux was neither accurately known nor negligible.

ECMWF analyzed vertical velocities represent an attractive way to try to fill this important data gap and were one major incentive for ASTEX to coordinate its observations closely with ECMWF. Figure 12 shows the 850 hPa vertical velocities averaged for 12 hours around 00Z June 13 and 00Z

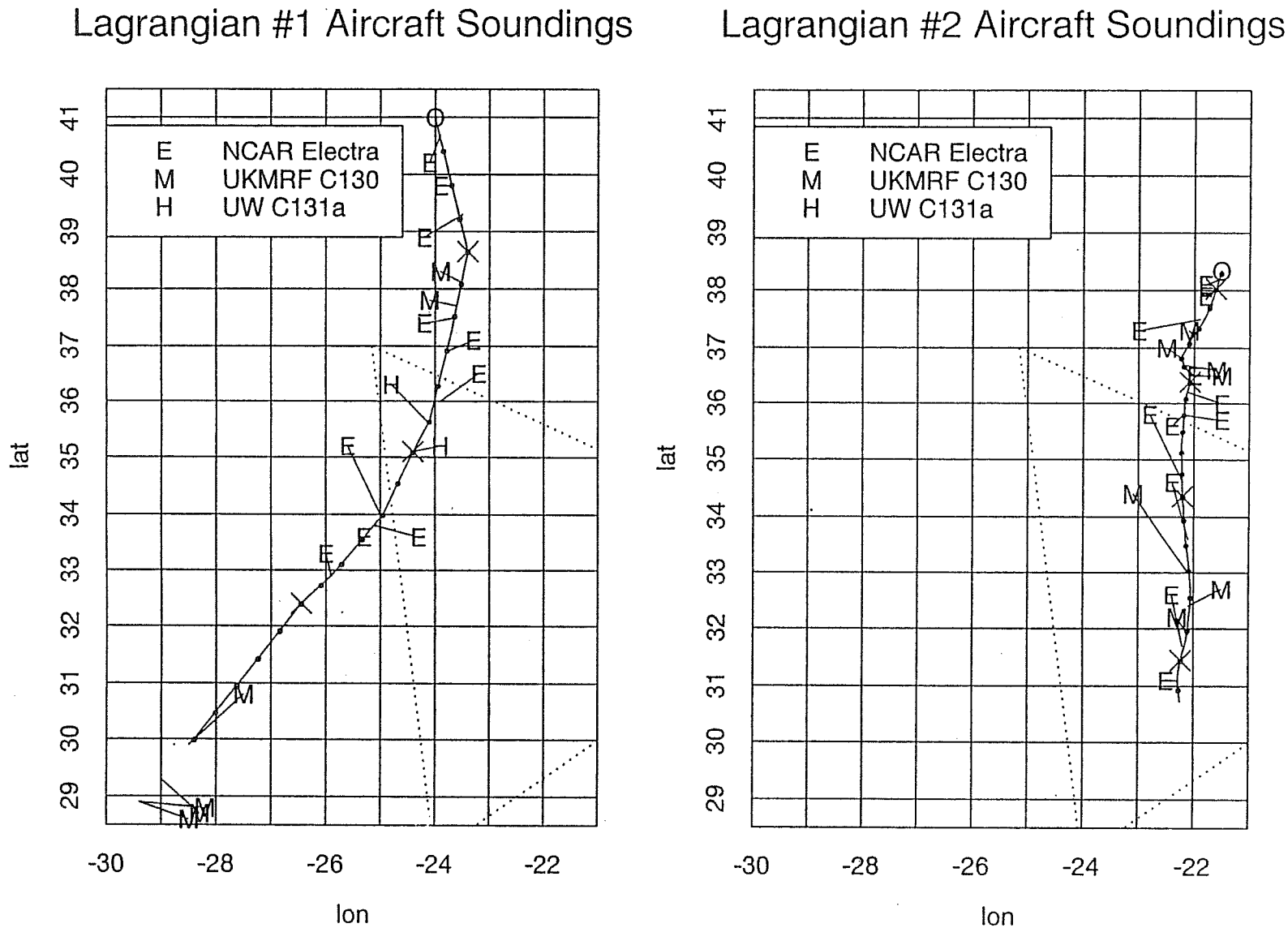

Fig. 9 Aircraft soundings during the two Lagrangians. The solid line on each picture is the estimated MBL air column trajectory and the ends of the line segments extending out from it indicate the positions of aircraft soundings. Each line segment is connected to the trajectory at the position corresponding to the sounding time. 'O' indicates the position of the R/V Oceanus when balloons were launched.

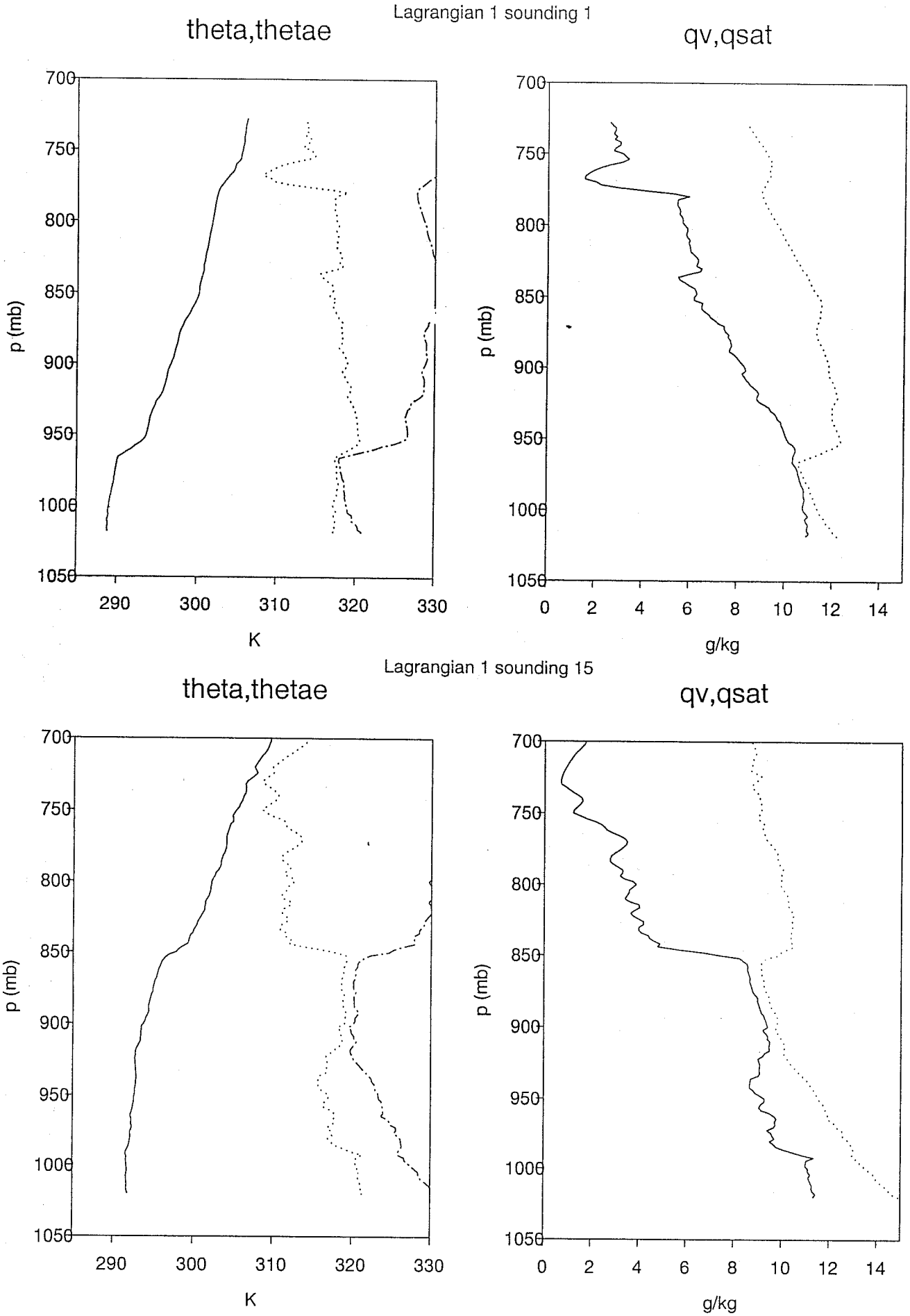

Fig. 10 Aircraft soundings 1 (N, W) and 15 from Lagrangian 1. On the left are θ (solid), θ_e (dots) and saturation θ_e (chain-dash). On the right are mixing ratio (solid) and saturation mixing ratio (dots).

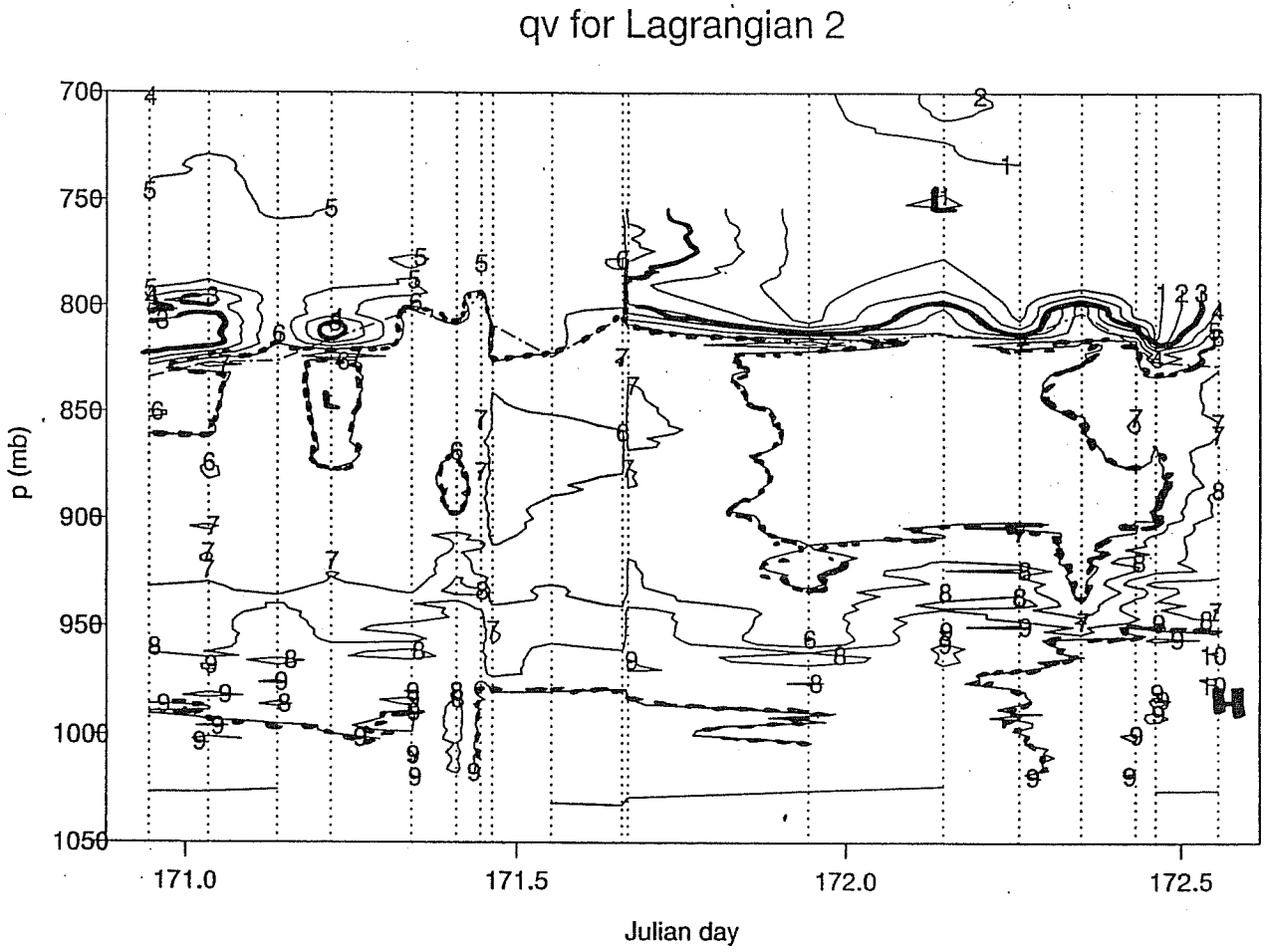

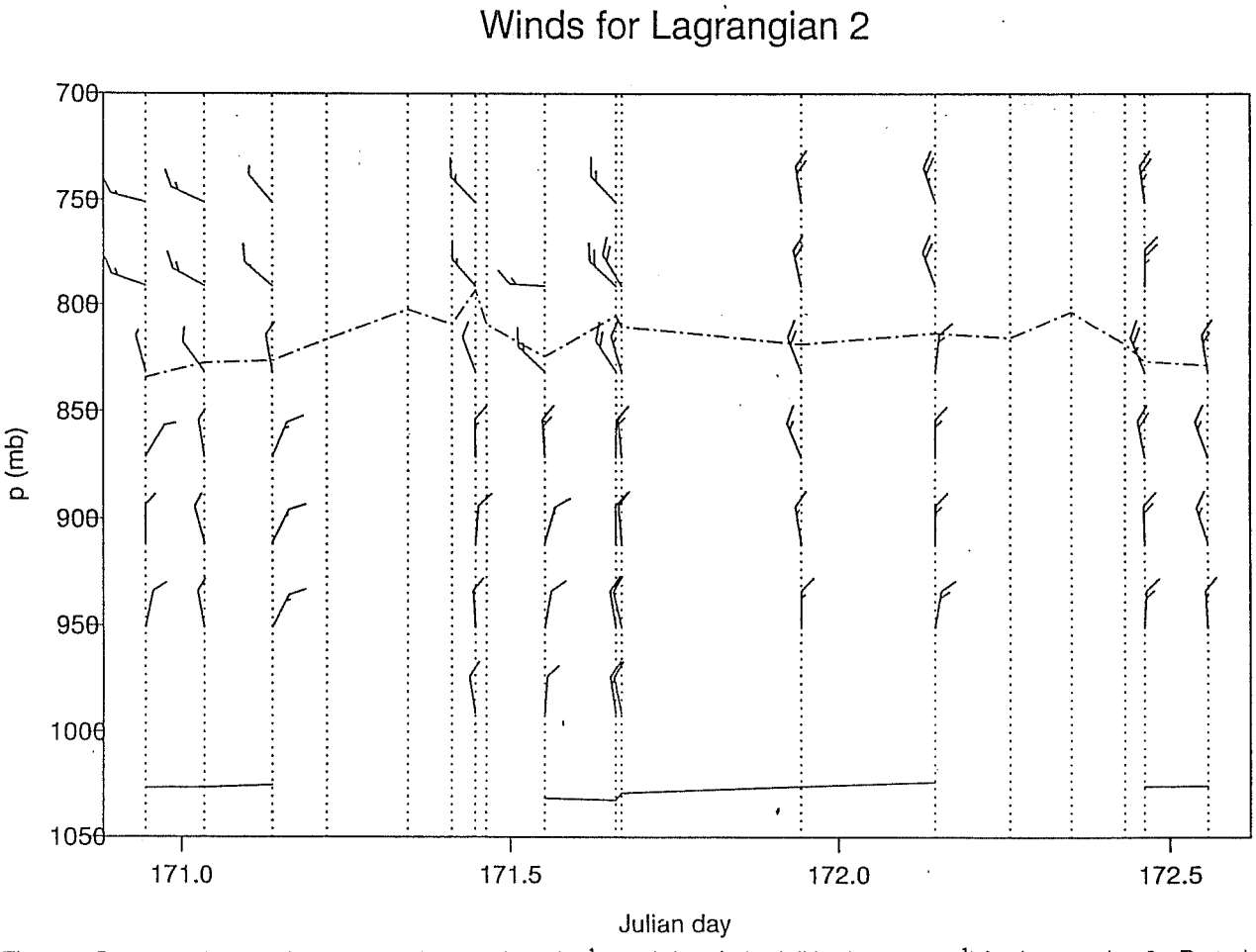

Fig. 11 Pressure-time sections of (a) mixing ratio (g kg^{-1}), and (b) winds (full barb = 5 m s^{-1}) for Lagrangian 2. Dotted vertical lines indicate times of soundings; wind soundings have only been analyzed for the Electra.

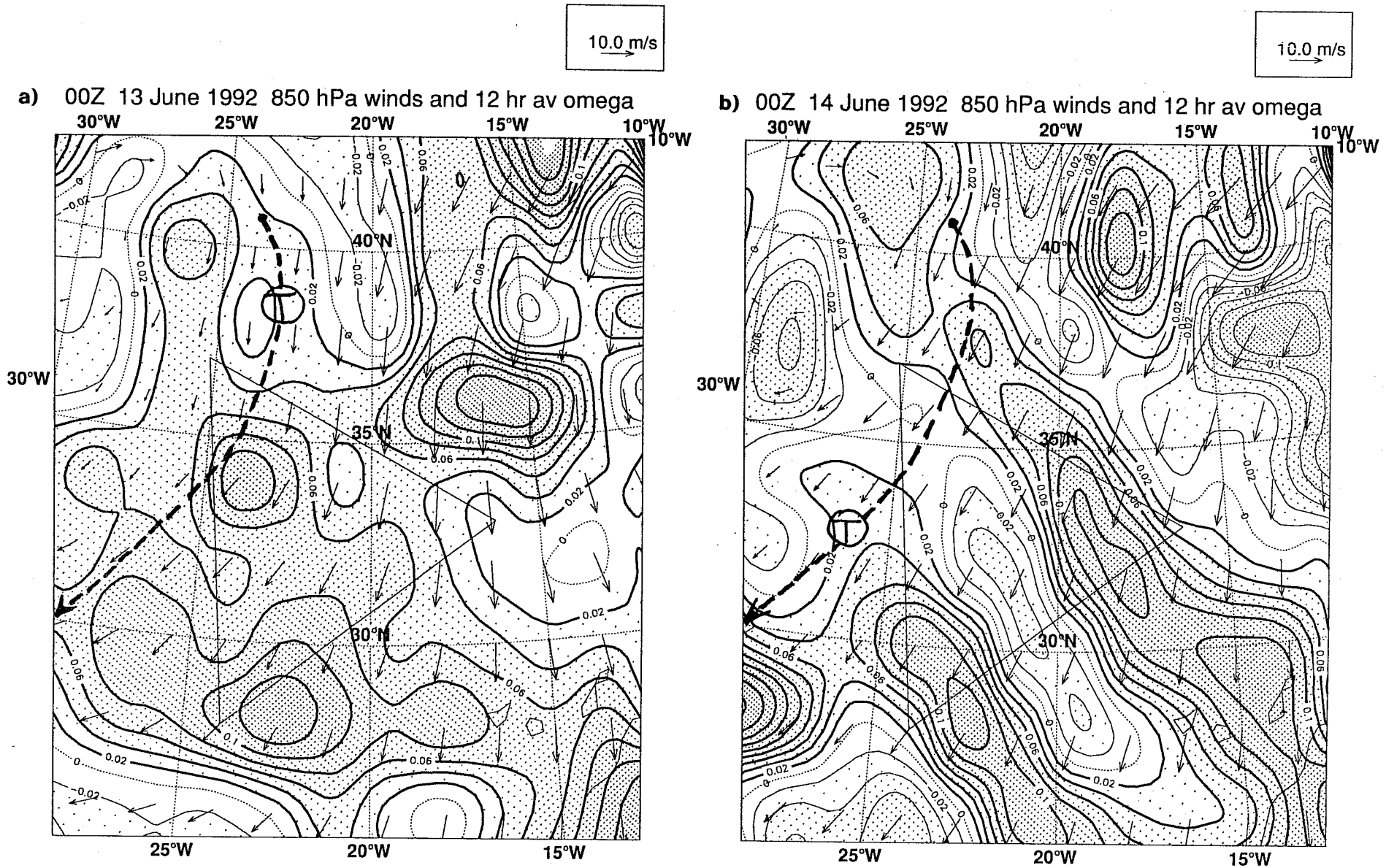

Fig. 12 850 hPa vertical velocities averaged for 12 hours around (a) 00Z June 13 and (b) 00Z June 14. In each case the trajectory is drawn and the air parcel position from Lagrangian 1 at the same time is demarkated with 'T'.

June 14, with the air parcel position from Lagrangian 1 overlaid. They vary substantially with position so that one cannot place too much confidence in the exact vertical velocities obtained (to better than a factor of two). This conclusion is corroborated by time series of ECMWF 850 hPa vertical velocity along the trajectory (not shown), which show large swings every 6-8 hours of 0.1 Pa s^{-1}, perhaps due to an imperfectly balanced initial state.

3. Large-Eddy Simulation of the STT

Although the focus of this paper is the ASTEX dataset, some recent simulations we have done with a large eddy simulation model developed at the University of Washington show quite striking similarities to the MBL structure found in ASTEX. The model uses a flux-limited Smolarkiewicz forward-in-time differencing scheme, and includes two-stream long and shortwave radiation parameterizations, surface fluxes, a Smagorinsky-type eddy diffusion, and allows for mean subsidence.

The goal of the simulations was to simulate the STT in as simple a set of forcing conditions as possible. Since 3 days of simulated time were simulated with a 2.5 second timestep, the model was run in two-dimensional mode with 100 m horizontal and 50 m vertical resolution, and a domain 4 km wide by 2.5 km high. Precipitation was suppressed for this run. A constant wind speed of 7 m s^{-1} and horizontal divergence of 2.5 x 10^{-6} s^{-1} was imposed, and a constant mixing ratio of 4 g kg^{-1} was assumed above the MBL. The initial temperature profile above the boundary layer was chosen to remain in radiative-subsidence balance so the temperature remained essentially constant above the MBL throughout the simulation. However, the sea surface temperature was increased at 1.5 K day^{-1}, and the MBL deepened from 900 m to 2000 m.

Figure 13 shows the liquid water and total water mixing ratios from this simulation at 10 a. m. local time on the three simulated days. On day 1, there is a 200 m thick, fairly uniform stratocumulus layer. Some evidence of diurnal decoupling (Turton and Nicholls 1987) is seem in the total water mixing ratio, which is 1 g kg^{-1} larger in the lowest 400 m, but eddies still penetrate the entire boundary layer depth. In the next two days, the subcloud layer moistens but the rest of the bound-

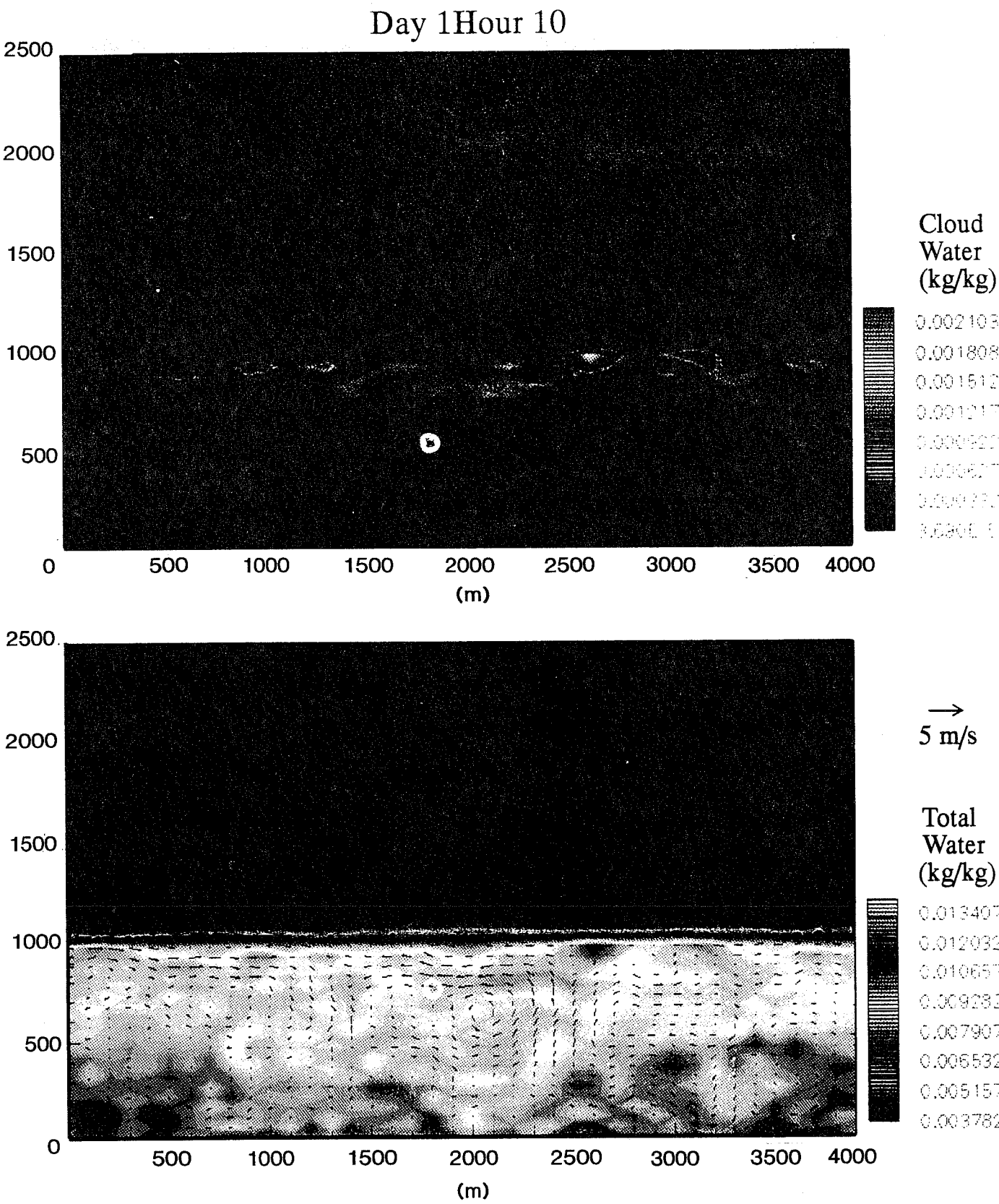

Fig. 13 (a) Liquid water (top) and total water mixing ratios (bottom) from this simulation at 10 am local time on day 1.

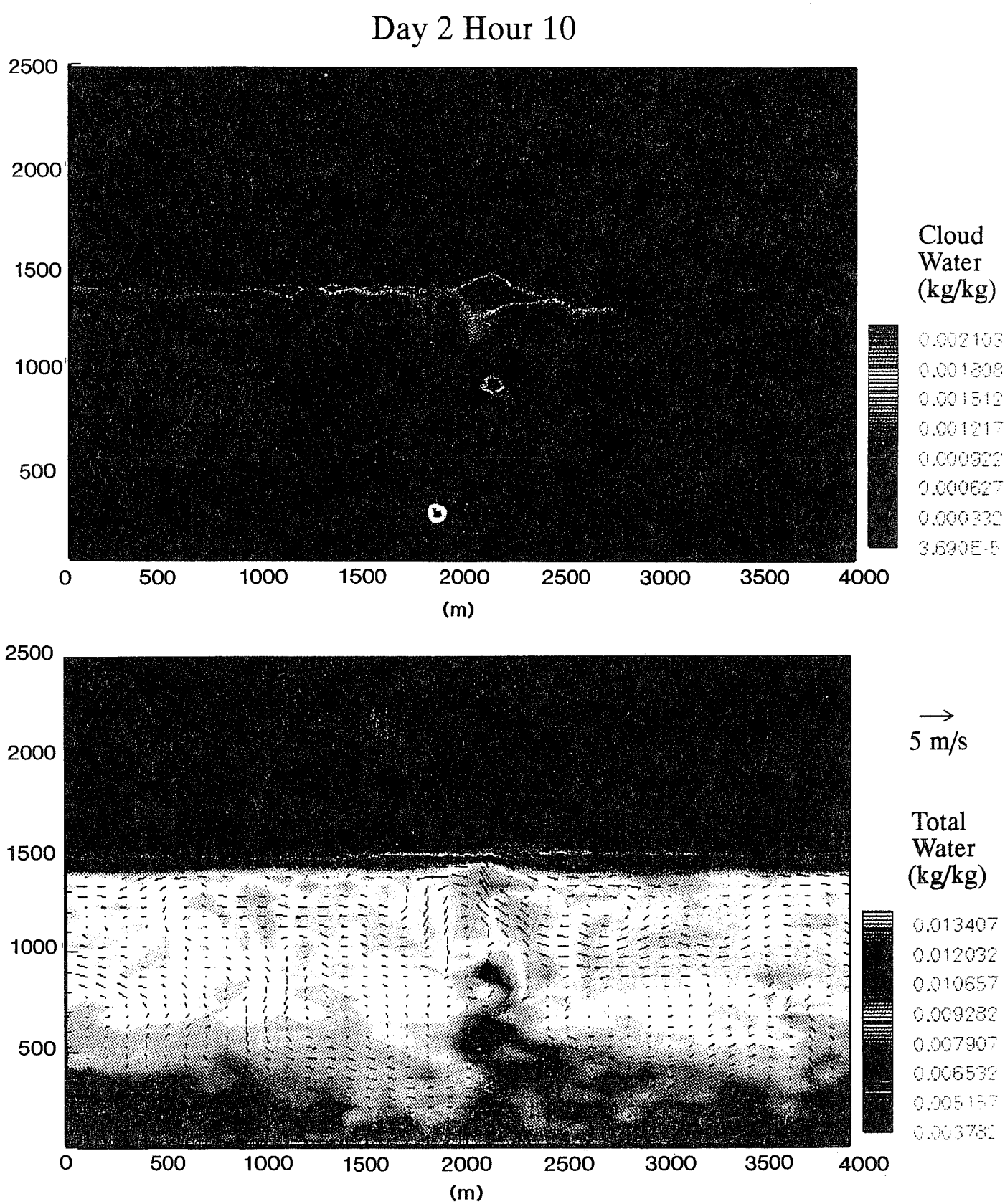

Fig. 13 (b) Liquid water (top) and total water mixing ratios (bottom) from this simulation at 10 am local time on day 2.

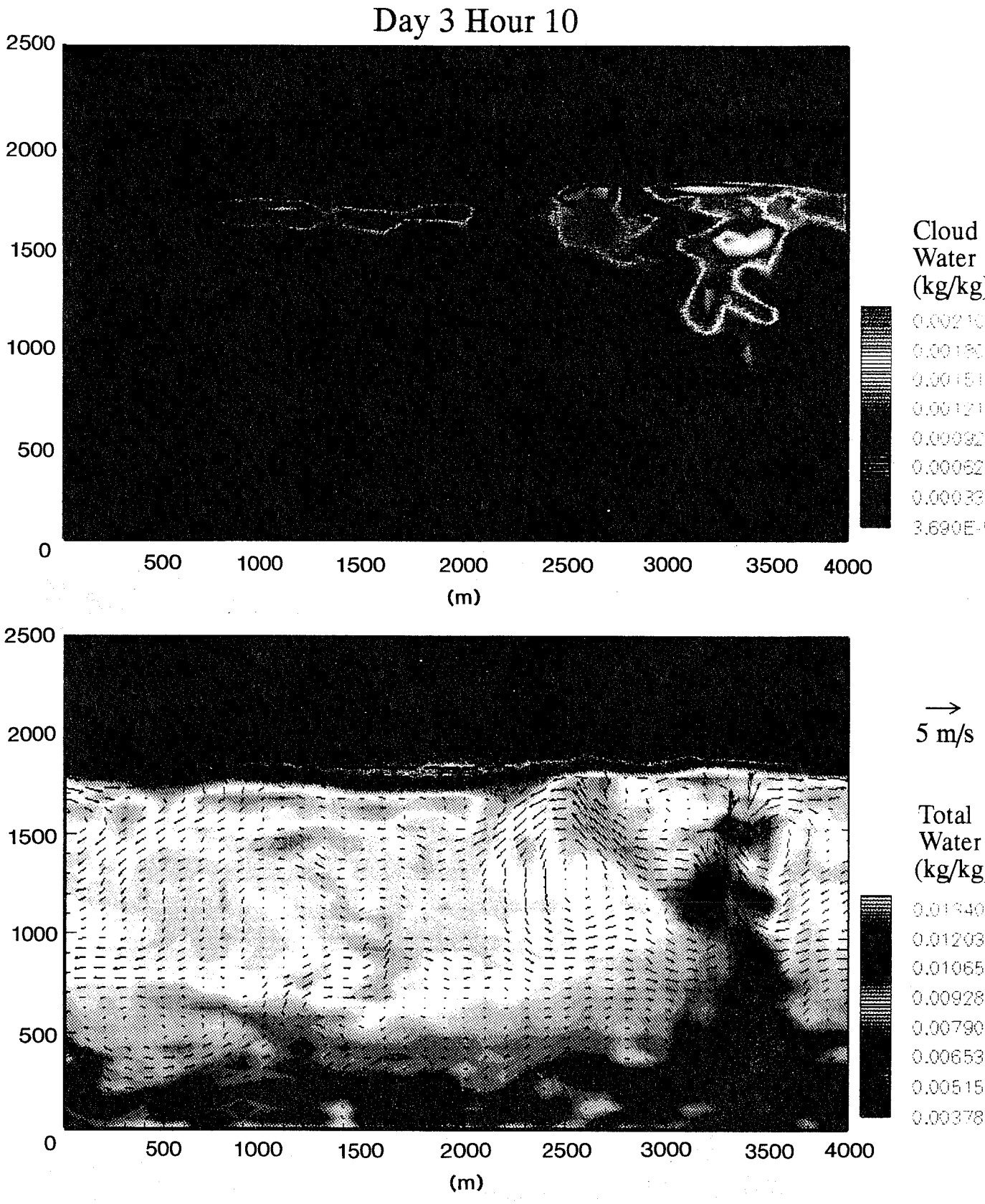

Fig. 13 (c) Liquid water (top) and total water mixing ratios (bottom) from this simulation at 10 am local time on day 3.

ary layer dries slightly. On day 2 a small cumulus cloud can be seen below the main stratus base; on day 3 a quite vigorous cloud with a 5 m s^{-1} updraft is seen. The total mixing ratio is fairly uniform above the cumulus base, an indication that little moisture detrainment is occurring between the transition layer and the inversion base. The stratification in this layer (not shown) is also quite weak, reflecting the fact that there must be a balance between a relatively small temperature tendency, almost negligible radiative cooling and adiabatic warming due to compensating subsidence around the cumuli. For the clouds to carry a substantial moisture flux to balance entrainment drying in the trade inversion, the cumulus mass flux must be substantial, yet the subsidence warming must be small--hence the stratification must be weak. The cloud fields on days 2 and 3 are strikingly similar to those seen in ASTEX in both depth and vertical structure. However, when this simulation is extended the upper stratocumulus layer does not appear to dissipate for realistic values of SST. This may be a result of insufficient turbulent entrainment by cumuli impinging on the inversion (which is almost entirely handled by the subgridscale turbulence parameterization), or perhaps of the neglect of precipitation; both of these are under investigation.

4. Conclusions

ASTEX provided a comprehensive dataset on marine boundary layer cloud in a regime intermediate between midlatitude and subtropical regimes. The MBL was characterized by substantial synoptic-scale variability in depth and cloudiness, and typically was a 'cumulus coupled' boundary layer with cumulus rising into a sheet of stratocumulus or 20-100 km broad stratocumulus patches. However, other cloud types such as fog and trade cumulus were also seen. The mean cloud cover varied between 40-70% in the triangle. Patchy drizzle was sometimes seen when the MBL was relatively clean. The ECMWF analyses of temperature and mixing ratio seem to been quite accurate at the sounding sites within the triangle, though preliminary indications are that the ECMWF diagnostic scheme for low-level cloud (slingo 1987) had little predictive value. It is probable that the type of MBL seen in the Atlantic is very common in the eastern subtropical Atlantic and Pacific Oceans and perhaps in summertime in the midlatitude oceans, wherever the boundary

layer is too deep to remain well-mixed.

Can a global model represent this kind of MBL structure with current vertical resolutions (25-50 hPa in the boundary layer)? Clearly, stratocumulus clouds, which are almost opaque to long-wave radiation even with thicknesses of as little as 10 hPa, and are usually between 10 and 40hPa thick, are not resolved. However, the decoupling of deeper MBL's is effectively achieved in the ECMWF model already by activating a stratocumulus parameterization for convective cloud layers one gridpoint thick and a cumulus parameterization for deeper cloud layers. Thus one must ask how well the shallow cumulus parameterization can predict the cloud at the inversion base, which may be less an issue of resolution than maintaining a correct mean sounding and of detraining appropriate amounts of liquid water from the cumulus clouds themselves. The ASTEX data will be an interesting test for shallow-convection schemes coupled with prognostic liquid water and cloud fraction such as that proposed by Tiedke (1993). Such schemes may also help us assess the global sensitivity of cloudiness to aerosol variability, which was so evident on a synoptic scale in ASTEX.

References

Augstein, E., H. Schmidt, and F. Ostapoff, 1974: The vertical structure of the atmospheric planetary boundary layer in undisturbed trade winds over the Atlantic Ocean. *Bound.-Layer Meteor.*, **6**, 129-150.

Betts, A. K., and B. A. Albrecht, 1987: Conserved variable analysis of the convective boundary layer thermodynamic structure over the tropical oceans. *J. Atmos. Sci.*, **44**, 83-99.

Bluth, R. T., and B. A. Albrecht, 1993: ASTEX and MAGE June 1992 Experiment Summary. Part I - Mission Summaries. Pennsylvania State University Department of Meteorology, 286 pp.

Klein, S. A., and D. L. Hartmann, 1993: The seasonal cycle of low stratiform clouds. *J. Climate*, to appear.

Malkus, J. S., 1958: On the structure of the trade wind moist layer. *Papers Phys. Oceangr. Meteor.*, **13**, No. 2, 47 pp.

Roach, W. T., R. Brown, S. J. Caughey, B. A. Crease and A. Slingo, 1982: A field study of nocturnal stratocumulus: I. Mean structure and budgets. *Quart. J. Roy. Meteor. Soc.*, **108**, 103-123.

Slingo, J. M., 1987: The development and verification of a cloud prediction scheme for the ECMWF model. *Quart. J. Roy. Meteor. Soc.*, **113**, 899-927.

Tiedke, M., 1993: Representation of clouds in large-scale models. Submitted to *Mon. Wea. Rev.*

Turton, J. D., and S. Nicholls, 1987: Diurnal variation of stratocumulus. *Quart. J. Roy. Meteor. Soc.*, **113**, 969-1009.